LCH

INSTITUT FOR BÆRENDE KONSTRUKTIONER OG MATERIALER

DTU

Shear Strength of Non-Shear Reinforced Concrete Elements

Part 3. Prestressed Hollow-Core Slabs

LINH CAO HOANG

DEPARTMENT OF STRUCTURAL ENGINEERING AND MATERIALS
TECHNICAL UNIVERSITY OF DENMARK Series R No 30 1997

Preface

The present work has been carried out at the Department of Structural Engineering and Materials, Technical University of Denmark, under the supervision of Professor, dr. techn. M.P. Nielsen.

I would like to thank my supervisor for giving valuable advice and inspiration as well as valuable criticism to the report.

Thanks are also due to my co-supervisors Assoc. Prof., lic.techn. Henrik Stang and lic.techn. Bent Feddersen.

Lyngby, July 1997.

Linh Cao Hoang

Summary

This paper deals with the shear strength of prestressed hollow-core slabs determined by the theory of plasticity. Two failure mechanisms are considered in order to derive the solutions.

In the case of sliding failure in a diagonal crack, the shear strength is determined by means of the crack sliding model developed by Jin-Ping Zhang [94.1]. The model takes into account the resistance against formation of cracks due to prestressing as well as the variation of the prestressing force in the transfer zone.

Due to the fact that the anchorage of the reinforcement takes place by bond, a rotation failure, which is induced by a crack formed at the support with subsequent slip of the reinforcement, is also considered. This failure mode is likely to occur in cases with a high prestressing force combined with a short shear span.

The theoretical calculations are compared with test results from the literature.

A good agreement has been found.

Resumé

Denne rapport behandler forskydningsbæreevnen af forspændte huldækelementer bestemt v.h.a. plasticitetsteorien. Løsningerne udledes udfra to brudmekanismer.

I de tilfælde, hvor der sker glidningsbrud i en diagonalrevne, bestemmes forskydingsbæreevnen ved hjælp af "crack sliding" modellen udviklet af Jin-Ping Zhang [94.1]. Modellen tager hensyn til forspændingens bidrag til modstanden mod revnedannelse såvel som variationen af forspændingskraften i overføringszonen.

Da forankringen af spændarmeringen sker ved hjælp af forskydningsspændinger mellem beton og armering er der i rapporten også behandlet det tilfælde, hvor et rotationsbrud opstår som følge af, at en revne dannes ved understøtningen hvorefter udtrækning af armeringen finder sted. Dette brud kan forekomme når en stor forspændingskraft kombineres med en kort spændvidde.

De teoretiske resultater sammenlignes med forsøgsresultater fra litteraturen.

Der er fundet god overensstemmelse.

Table of Contents

Preface i

Summary ii

Notations vi

1. Introduction 1

2. Prestressed beams with bond anchorage 3

2.1 Sliding failure 3

2.2 Rotation failure 10

2.3 Transfer length 13

3. Prestressed hollow core-slabs 15

3.1 Sliding failure 17

3.2 Rotation failure 22

4. Comparison with test results 24

4.1 Tests from Delft University of Technology 25

4.2 Tests from CBR in Belgium 26

4.3 Tests from Einhoven University of Technology 28

4.4 Tests from Dansk Spændbeton 30

4.5 Comparison with all tests 33

5. Conclusion 34

References 35

Appendix A

Appendix B

Appendix C

Appendix D

Notations

a : Shear span

a/h : Shear span ratio

A_c : Area of concrete cross section

$A_{c,ef}$: Area of effective concrete cross section

A_p : Area of prestressing reinforcement

b_f : Width of flange

b_w : Width of web

e : Distance from the top face to the center of gravity of the cross section

f_c : Uniaxial compressive strength of concrete

f_p : Yield strength of prestressing reinforcement

f_{tef} : Effective plastic tensile strength of concrete

$F(x')$: Prestressing force in the transfer zone

F_{se} : Effective prestressing force outside the transfer zone

h : Depth of beam/slab

h_e : Effective depth of beam/slab

l_t : Transfer length

$M_{c,cr}$: Moment around the upper tip of a crack (contribution from the concrete)

$M_{s,cr}$: Moment around the upper tip of a crack (contribution from the prestressing force)

n : Number of cavities in the slab

s : Length of support plate

$s(h)$: Size effect parameter

t : Thickness of flange

t_o : Thickness of compression flange

t_u : Thickness of tension flange

u : Relative displacement in yield line

V : Reaction at support / shear force

V_{cr} : Cracking load

V_u : Ultimate load/shear force

V_{test} : Observed ultimate shear force in test

$V_{cal.}$: Calculated ultimate shear force

x : Horizontal projection of critical diagonal crack / yield line

x' : $=a - x$

ϕ : Diameter of prestressing strand

ν_0 : Effectiveness factor

θ : Rotation angle

ρ : Reinforcement ratio ($=A_p/A_c$)

τ : Shear stress

τ_c : $=0.059\nu_0 f_c$

τ_u : Shear capacity ($= V_u/b_w h$)

Chapter 1

Introduction

This paper deals with the shear strength of prestressed hollow-core slabs. The reason for taking up this subject is that the application of prestressed hollow-core slabs has greatly increased over the last decades.

Many methods regarding the shear analysis of prestressed hollow-core slabs have been proposed, see e.g. [79.1], [82.1], [83.1] and [94.2]. Common for the methods proposed is that they draw heavily upon the theory of elasticity, neglecting the fact that the theory of plasticity has proved its applicability in the limit state analysis of a wide range of problems in structural concrete.

In the case of prestressed hollow-core slabs, shear failure and anchorage failure are very likely to occur due to the configuration of the elements and the production method.

The presence of cavities obviously reduces the shear capacity. Further, the technique of extrusion, which is used in the production of hollow-core slabs, makes it impossible to provide the slabs with stirrups or to provide anchorage arrangement for the prestressing reinforcement.

Thus we are certainly dealing with rather primitive structural elements.

Recently a method to calculate the shear strength of non shear reinforced concrete beams has been developed by Jin-Ping Zhang [94.1]. The so-called crack sliding model is based upon the upper bound theorem of the theory of plasticity. This model assumes that the cracking of concrete introduces potential yield lines which, due to a reduced sliding resistance in the cracks, may be more dangerous than the yield lines predicted by the usual plastic theory.

Description and applications of this model may be found in [94.1] and [97.2].

In this paper we shall demonstrate how the crack sliding model may be applied to prestressed elements with anchorage by bond of the prestressing reinforcement. It will be shown how the prestressing force as well as the transfer length may be taken into account in a rational way.

Chapter 2
Prestressed Beams with Anchorage by Bond

Before treating the prestressed hollow-core slabs, we shall describe the basic principles of the crack sliding model by applying it to a simple case, namely a prestressed beam with rectangular cross section.

2.1 Sliding failure

Let's consider the prestressed simply supported beam shown in figure 2.1. The beam, which is not provided with shear reinforcement, is assumed to be overreinforced with the prestressing reinforcement area A_p. Furthermore, it is assumed that the reinforcement is anchored by bond near the beam ends.

The effective prestressing force F_{se} then has to be transferred to the concrete by bond over a certain transfer length l_t. Often, see e.g. [79.1], [82.1], [83.1], [94.2], the prestressing force is assumed to develop according to a parabolic curve. For simplicity, however, we will consider the prestressing force to vary linearly in the transfer zone, see figure 2.1. Details about the transfer length may be found in section 2.3.

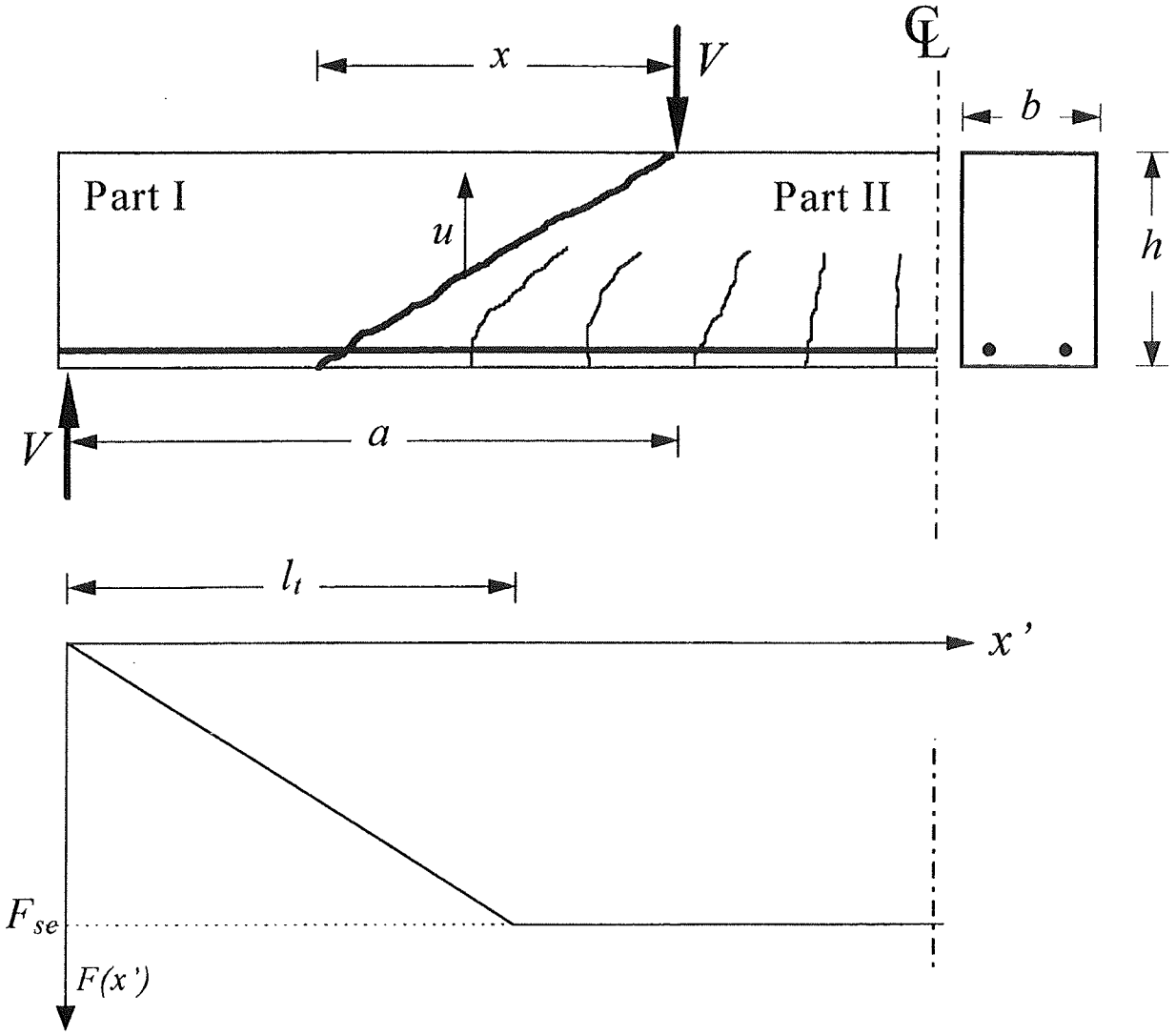

Figure 2.1 *Prestressed beam with anchorage by bond.*

Shear failure is assumed to take place as sliding in a critical diagonal crack which ends at the loading point. The horizontal projection of the critical diagonal crack, which is denoted as x, is found by the following equation, see [94.1] and [97.2],

$$V_u = V_{cr} \tag{2.1}$$

Here V_{cr} is the load needed to form the crack and V_u is the load needed to

cause sliding in the same crack.

Due to the assumption of overreinforcement, the motion of part I relative to part II will be vertically directed. This of course implies that the anchorage of the reinforcement is assumed to be strong enough to maintain equilibrium after formation of the diagonal crack. In this section we assume this condition to be fulfilled. The problem of slip of the reinforcement bars is treated in the next section.

The crack sliding capacity may be determined by the following approximation to the correct work equation, see [97.1] and [97.2],

$$V_u \cdot u = 2\frac{\tau_c}{\frac{x}{h}} A_c \cdot u \tag{2.2}$$

Here A_c is the area of the cross section and τ_c is given by the formula

$$\tau_c = 0.059 \nu_0 f_c \tag{2.3}$$

f_c being the uniaxial compressive strength of concrete and ν_0 is the effectiveness factor which may be taken as, see [94.1] and [97.2],

$$\nu_0 = 0.88\frac{1}{\sqrt{f_c}}\left(1+\frac{1}{\sqrt{h}}\right)(1+26\rho) \tag{2.4}$$

Here f_c is the compressive strength of concrete in MPa, h is the absolute depth of the beam in m and ρ is the reinforcement ratio.

The diagonal crack may be formed when the load level is high enough to exceed the effective tensile strength of concrete as well as the prestressing force, see the illustration in figure 2.2. By a rotation mechanism around the upper tip of the crack, V_{cr} may be determined by the following work equation, see also [94.1] and [97.2],

$$V_{cr} \cdot a = M_{c,cr}(x) + M_{s,cr}(x') \tag{2.5}$$

Here $M_{c,cr}(x)$ and $M_{s,cr}(x')$ represent the resistance against crack formation from the concrete and the prestressing reinforcement, respectively. $M_{c,cr}(x)$ and $M_{s,cr}(x')$ are determined by a moment equation around point O, see figure 2.2. Thus the prestressing force $F(x')$ is taken into account as an external normal force.

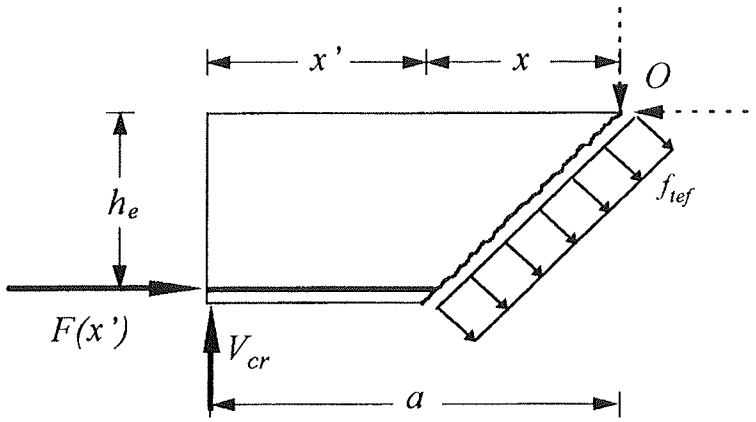

Figure 2.2 *Stress distribution in a developing crack.*

For any shape of cross section $M_{c,cr}(x)$ may be determined as

$$M_{c,cr}(x) = f_{tef} \cdot A_c \cdot e \cdot \left(\left(\frac{x}{h} \right)^2 + 1 \right) \tag{2.6}$$

Here A_c is the area of the concrete cross section and e is the distance from the upper face to the centre of gravity of the cross section. In the case of a rectangular cross section A_c and e assumes the values bh and $\frac{1}{2}h$, respectively. The effective plastic tensile strength may be taken as, see [94.1],

$$f_{tef} = 0.156 \cdot f_c^{2/3} \cdot s(h) \qquad (f_c \text{ in MPa}) \tag{2.7}$$

In this formula the function $s(h)$ takes into account size effects. This function may be chosen to be

$$s(h) = \left(\frac{h}{0.1}\right)^{-0.3} \qquad (h \text{ is the depth of beam in meter}) \tag{2.8}$$

The resistance against crack formation furnished by the prestressing force may be found by the moment equation

$$M_{s,cr}(x') = F(x') \cdot h_e \tag{2.9}$$

Here $F(x')$ is the effective prestressing force in the distance x' from the support (the length of the support plate is disregarded). By utilising that $x' = a - x$, we may rewrite (2.9) as follows[1)]

$$M_{s,cr} = \begin{cases} F_{se} \dfrac{a-x}{l_t} \cdot h_e & , \text{ for } a - x < l_t \\ F_{se} \cdot h_e & , \text{ for } a - x \geq l_t \end{cases} \tag{2.10}$$

The horizontal projection of the critical diagonal crack may now be found by inserting (2.2) and (2.5) into (2.1). The shear capacity, expressed as an average shear stress $\tau_u = V_u/bh$, may then be found by

$$\tau_u = 2\frac{\tau_c}{\frac{x}{h}} \tag{2.11}$$

The solution of equation (2.1) must be determined numerically. The validity of the solution must of course be checked. This may be done in the following way.

First the upper formula of (2.10) is inserted into (2.1). If the solution satisfies the condition $x > a - l_t$ then the solution is valid. Otherwise the lower

---

[1)] To be correct, the prestressing force must in fact be taken at the point $x' + (h - h_e)x/h$. For simplicity, however, the last term may be disregarded without introducing any significant error.

formula of (2.10) must be inserted into (2.1) in order to find the horizontal projection x of the yield line.

Furthermore, it must be checked that x is less than a, otherwise the yield line is not geometrically possible. If x is found to be larger than a, then the shear capacity may be found as explained in the next section.

The basic features of the crack sliding model are illustrated in figure 2.3 showing the variation of V_u and V_{cr} with x. The horizontal projection of the diagonal crack transformed into a yield line is determined by the point of intersection between the two curves.

The dotted curve represents the cracking load with no prestressing. It appears that the only change caused by prestressing is that the cracking load is increased by a function which is affine to the shape of the prestressing force curve.

In figure 2.3 the point of intersection is shown outside the transfer zone. Of course the point of intersection may also lie within this zone.

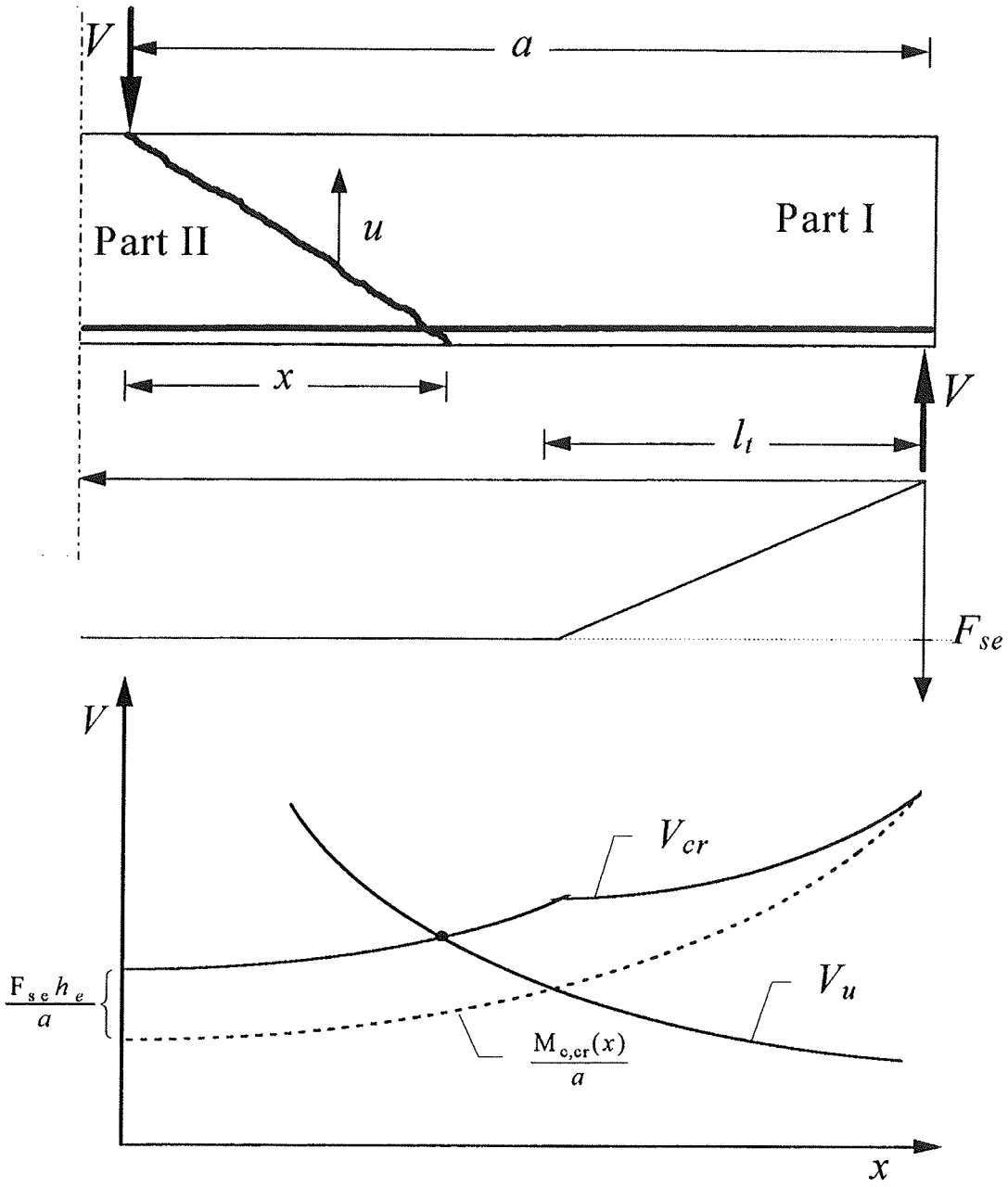

Figure 2.3 *Determination of the horizontal projection x of the diagonal crack.*

2.2 Rotation failure

Since the prestressing reinforcement is not anchored at the beam ends, slip of reinforcement can not always be avoided. Therefore an additional failure criterion, which is associated with a diagonal crack, must be included in the shear analysis.

When a large prestressing force is combined with a short shear span, it might happen that a diagonal crack originating from the support will form at a lower load level than the load level corresponding to the point of intersection between the cracking load curve and the crack sliding capacity curve.

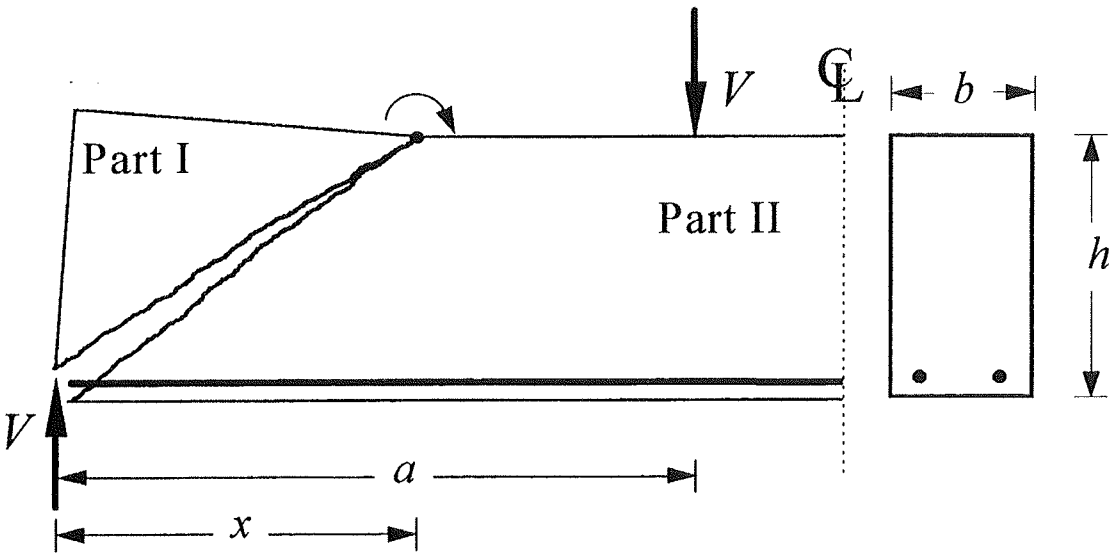

Figure 2.4 *Rotation failure.*

In this case a rotation around the upper tip of the crack will immediately take place due to the lack of end anchorage. The ultimate load may be found from the following work equation, see figure 2.4,

$$V_u \cdot x = f_{tef} \cdot A_c \cdot e \cdot \left(\left(\frac{x}{h} \right)^2 + 1 \right) \tag{2.12}$$

By minimising V_u with respect to x, it is easily verified that a minimum is

found for $x = h$. Thus, the bearing capacity corresponding to a rotation failure mechanism is given as

$$V_u = 2 \cdot f_{tef} \cdot A_c \cdot \frac{e}{h} \tag{2.13}$$

In the particular case of a rectangular cross section, V_u assumes the value bhf_{tef}. It is interesting to notice that the shear strength of the beam can never exceed this value if there is no anchorage at the ends of the beam.

It is also interesting to notice, that beyond a certain level of prestressing, it is no longer beneficial to increase the prestressing force. This situation is illustrated in figure 2.5, where two cracking load curves corresponding to two different prestressing levels are shown.

At the prestressing level corresponding to $F_{se,1}$, it appears that the shear capacity, determined by the intersection point of V_u and $V_{cr}(F_{se,1})$, is lower than the one given by (2.13). Thus, the shear capacity in this case will correspond to the point of intersection.

In the other case with the prestressing level $F_{se,2}$, the point of intersection leads to a shear capacity which is higher than the one given by (2.13). Hence, the shear capacity is determined by (2.13) and it appears that a higher prestressing level will not increase the shear capacity.

The only way of finding out, which of the two failure mechanisms gives the lowest shear capacity, is to perform both calculations.

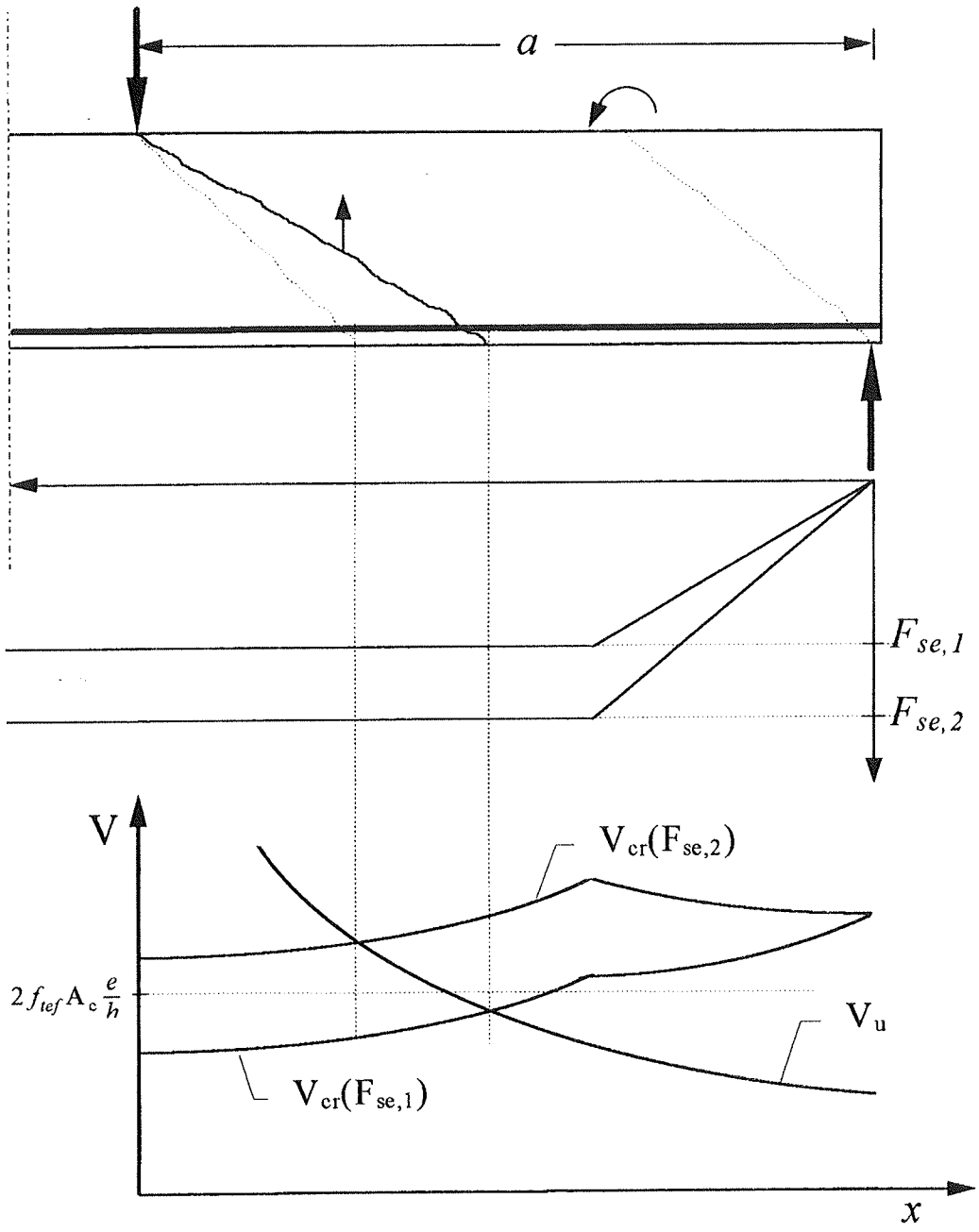

Figure 2.5 *Shear capacity corresponding to different prestressing levels.*

2.3 Transfer length

It appears from the preceding sections that the need of a transfer length introduces an important difference between the analysis of beams with and without end anchorage.

Many expressions for the transfer length have been proposed, but the problem is far from being fully clarified. The bond transfer is a complex problem and displays dependence on many parameters, such as the type of loading, the configuration of the surrounding concrete, the size and type of the reinforcement, etc.

This complexity makes it difficult, if not impossible, to determine the transfer length analytically. Therefore empirical rules based upon experimental results are necessary. The following is restricted to reinforcement bars in the form of strands.

We will adopt the simple expression given in a FIP-recommendation from 1988 and referred to in [94.2]

$$l_t = \begin{cases} 55\phi & \text{for slow release of strands} \\ 60\phi & \text{for rapid release of strands} \end{cases} \tag{2.14}$$

Here ϕ is the diameter of the strand.

A phenomenon, which always occurs at the ends of the beam, is the initial bond slip of the strands. The slip length is about $5\phi - 10\phi$, see [96.2], depending on how the strands are released. Rapid release will increase the slip length due to dynamic effects.

However, to simplify as much as possible, we neglect the initial slip.

In fact it can even be argued that this simplification is reasonable. The argu-

ment is as follows:

In the preceding sections we have disregarded the length of the support plate and we have assumed the prestressing force to be built up from the point of the resultant of the reaction. Since the length of the support plate is in the range of $10\phi - 20\phi$, then the resultant of the reaction will be in a distance of $5\phi - 10\phi$ from the end of the beam. This corresponds to the distance at which the prestressing force will begin to build up, if both the slip length and the support length are taken into account.

Chapter 3

Prestressed Hollow-Core Slabs

On the basis of the previous chapter, we may now derive the formulas for the shear capacity of prestressed hollow-core slabs. Although the principles are the same, some additional considerations must be made due to the presence of the voids.

In what follows we shall consider an idealised hollow-core slab with rectangular voids, see figure 3.1. The cross section of the hollow-core slab is composed of a number of unit cross sections with I-shape. The number of unit cross sections is equal to the number of voids, which we denote as n. The dimensions of the unit cross section are shown in the figure where b_w and b_f denote the web width and flange width, respectively. The thickness of the compression flange and the tension flange are denoted as t_o and t_u, respectively.

The formulas derived in this chapter may be applied to hollow-core slabs with any shape of the voids. When inserting into the formulas, t_o and t_u should be taken as the thinnest parts above and below the voids respectively and b_w should be put equal to the thinnest part between two voids.

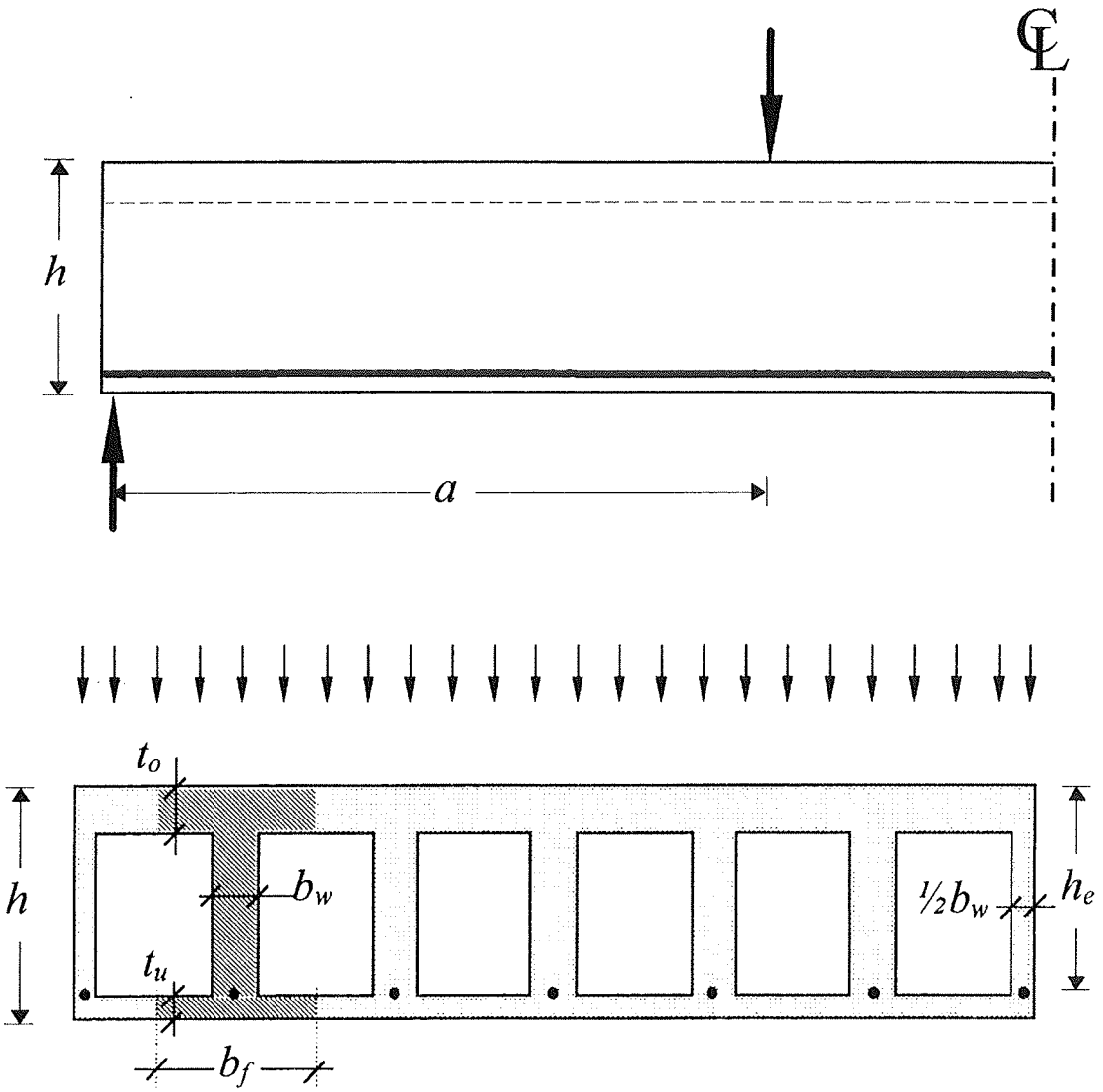

Figure 3.1 *Idealised hollow-core slab with rectangular voids.*

3.1 Sliding failure

In reference [97.3] which deals with the shear strength of T-beams, it was argued that the shear strength will be overestimated if crack sliding is assumed to take place in a crack running all the way through to the top face.

On the other hand, good agreement with test results was found when the shear capacity was derived from a failure mechanism involving crack sliding in the web and a kind of membrane action in the compression flange, see [97.3]. The failure mode is shown in figure 3.2.

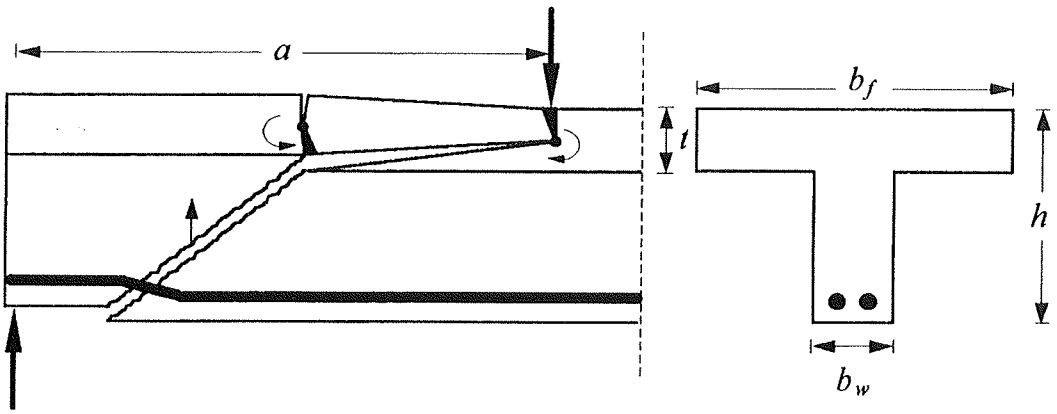

Figure 3.2 *Failure mechanism for beam with un-reinforced compression flange.*

It turns out from the investigations in [97.3], that the shear capacity of a T-beam may be found by multiplying a factor K (K = 1.08t/h +0.86) on the shear capacity of a similar beam with the rectangular cross section $b_w h$. The factor K only depends on the ratio between the flange thickness and the overall depth.

It is reasonable to believe that a similar, but not necessarily identical, rule may be applied to the case of a prestressed hollow-core slabs. However, for elements with thin compression flanges, i.e. t/h is about 0.15 - 0.2, the factor K does not increase the shear capacity significantly. Further, since the flanges in most hollow-core slabs are relatively thin, we shall disregard the

compression flange and assume the factor K to be unity.

Regarding the tension flange, it is reasonable to expect that crack sliding will take place here because cracks obviously are present in the tension flange at failure. Thus, the tension flange and the web can be treated on the same footing.

It follows from the discussion above, that we may determine the shear capacity of a hollow-core slab by disregarding the compression flange.

The effective cross section, which is to be considered, is shown in figure 3.3.

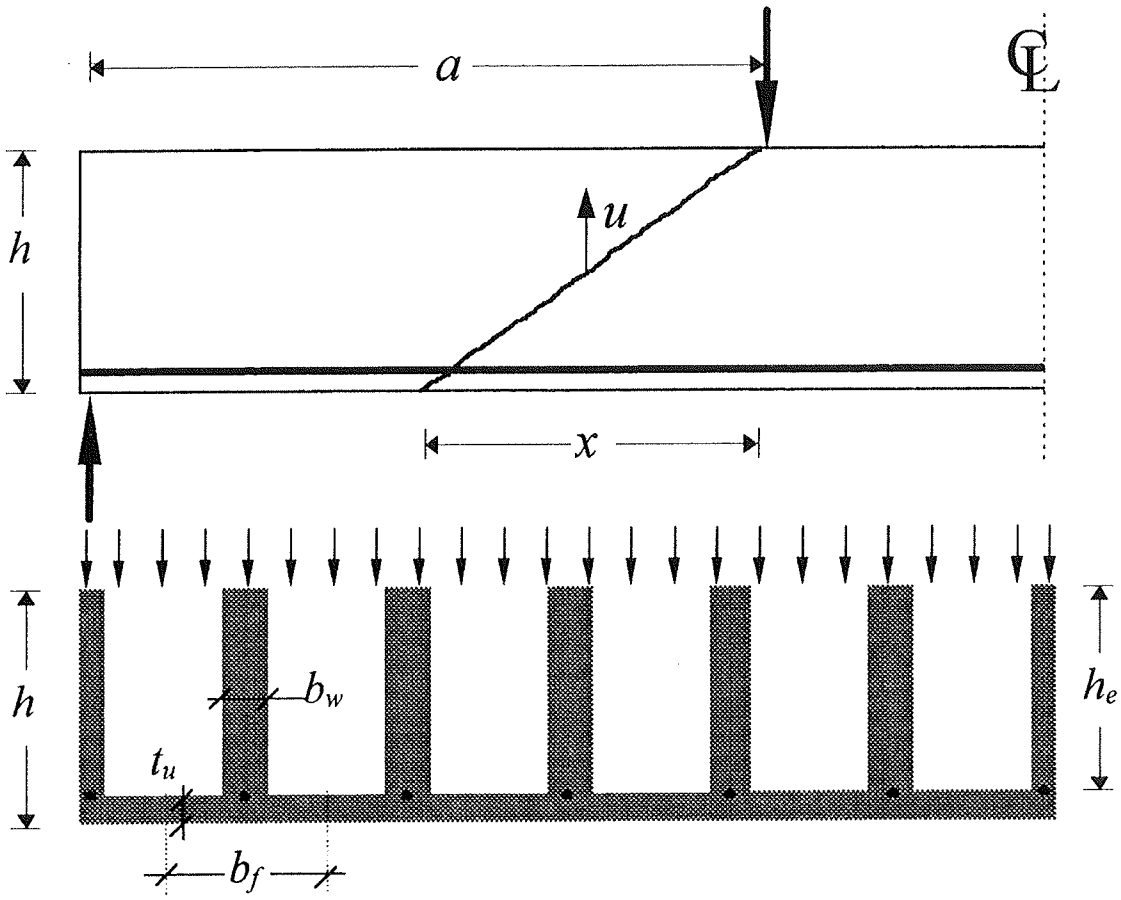

Figure 3.3 *Effective cross section of hollow-core slab in the case of sliding failure.*

The shear capacity, expressed as the total reaction V_u at failure, is determined as follows:

When sliding takes place in the critical diagonal crack with the horizontal projection x and when the relative displacement is vertically directed, we may find V_u as, see (2.2),

$$V_u = 2\frac{\tau_c}{\frac{x}{h}} A_{c,ef} \tag{3.1}$$

Here $A_{c,ef}$ is the effective cross section area which is given as

$$A_{c,ef} = n \cdot \left(t_u \cdot b_f + \left(h - t_u \right) \cdot b_w \right) \tag{3.2}$$

where n denotes the number of voids in the slab.

It should be noticed that in the formula for the effectiveness factor (2.4), the reinforcement ratio ρ has been inserted as

$$\rho = \frac{A_p}{A_{c,ef}} \tag{3.3}$$

Referring to (2.5), (2.6) and (2.10) we may find the cracking load V_{cr} as follows

$$V_{cr} = \begin{cases} \dfrac{f_{tef} \cdot A_{c,ef} \cdot \dfrac{e}{h} \cdot \left(\left(\dfrac{x}{h} \right)^2 + 1 \right) + F_{se} \dfrac{\left(\dfrac{a}{h} - \dfrac{x}{h} \right)}{\dfrac{l_t}{h}} \cdot \dfrac{h_e}{h}}{\dfrac{a}{h}}, & \text{for } a - x < l_t \\ \dfrac{f_{tef} \cdot A_{c,ef} \cdot \dfrac{e}{h} \cdot \left(\left(\dfrac{x}{h} \right)^2 + 1 \right) + F_{se} \cdot \dfrac{h_e}{h}}{\dfrac{a}{h}}, & \text{for } a - x \geq l_t \end{cases} \tag{3.4}$$

In this particular case, the distance from the upper face to the centre of gravity of the effective cross section is determined by the formula

$$e = \frac{0.5 \cdot b_w (h - t_u)^2 + b_f \cdot t_u (h - 0.5 \cdot t_u)}{b_f \cdot t_u + b_w (h - t_u)}$$

The horizontal projection of the critical diagonal crack may now be found by equalising (3.1) and (3.4), i.e.,

$$V_u = V_{cr} \tag{3.5}$$

When (3.1) and (3.4) is inserted into (3.5) we find the following two cubic equations rendering x/h :

$$\frac{e}{h}\left(\frac{x}{h}\right)^3 - \frac{h_e}{l_t}\frac{F_{se}}{f_{tef} A_{c,ef}}\left(\frac{x}{h}\right)^2 + \left(\frac{e}{h} + \frac{h_e}{l_t}\frac{a}{h}\frac{F_{se}}{f_{tef} A_{c,ef}}\right)\frac{x}{h} - \frac{2\tau_c}{f_{tef}}\frac{a}{h} = 0 \tag{3.6a}$$

$$\frac{e}{h}\left(\frac{x}{h}\right)^3 + \left(\frac{e}{h} + \frac{h_e}{h}\frac{F_{se}}{f_{tef} A_{c,ef}}\right)\frac{x}{h} - \frac{2\tau_c}{f_{tef}}\frac{a}{h} = 0 \tag{3.6b}$$

The solution to (3.6a) is valid if it satisfies the following condition

$$\frac{a}{h} > \frac{x}{h} > \frac{a}{h} - \frac{l_t}{h} \tag{3.7}$$

If (3.7) is not fulfilled then the horizontal projection must be found from (3.6b). In this case the solution must fulfil the requirement

$$\frac{x}{h} \leq \frac{a}{h} - \frac{l_t}{h} \tag{3.8}$$

When x/h is found the shear capacity related to a sliding failure may be determined by inserting into (3.1).

Of course it may happen that none of the conditions (3.7) and (3.8) can be brought into fulfilment, e.g. in cases with very high prestressing level and short shear spans. These cases are treated next.

3.2 Rotation failure

As described in chapter 2, a rotation failure may take place in cases with a high prestressing force combined with a short shear span. Figure 3.4 shows an example of this failure mode. It is evident that this failure was caused by crack opening and not crack sliding.

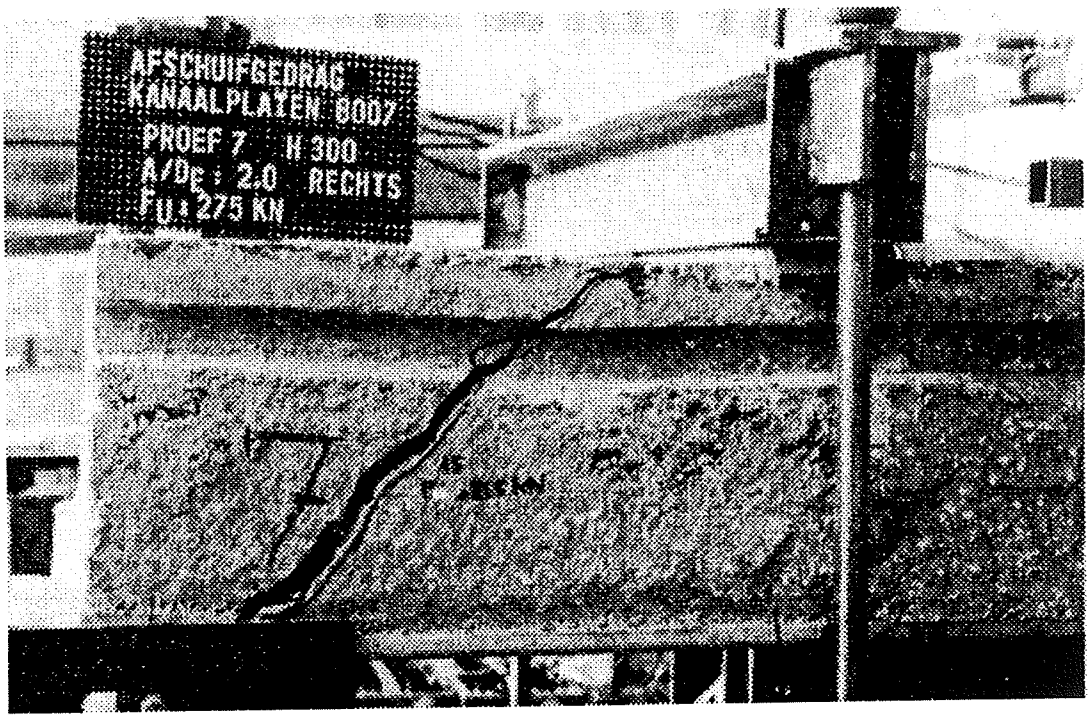

Figure 3.4 *Rotation failure* [*83.1*].

In this case both flanges may be taken into account because the crack obviously runs all the way through to the top face. However, the top flange do not contribute significantly due to the short lever arm.

The cross section area A_c and the distance e to the centre of gravity of the cross section may be determined as, see also figure 3.5,

$$A_c = n \cdot \left((t_o + t_u) \cdot b_f + (h - t_u - t_o) \cdot b_w \right) \tag{3.9}$$

$$e = \frac{0.5 \cdot \left(b_w (h - t_u)^2 + \left(b_f - b_w\right) t_o^2\right) + b_f (h - 0.5 \cdot t_u) t_u}{b_f \cdot t_o + b_f \cdot t_u + b_w (h - t_u - t_o)} \tag{3.10}$$

The shear strength related to a rotation mechanism is given by the following simple expression, see also (2.13),

$$V_u = 2 \cdot f_{tef} \cdot A_c \cdot \frac{e}{h} \tag{3.11}$$

In the special case of $t_o = t_u$ we have $e = 0.5h$. Thus, $V_u = f_{tef} A_c$.

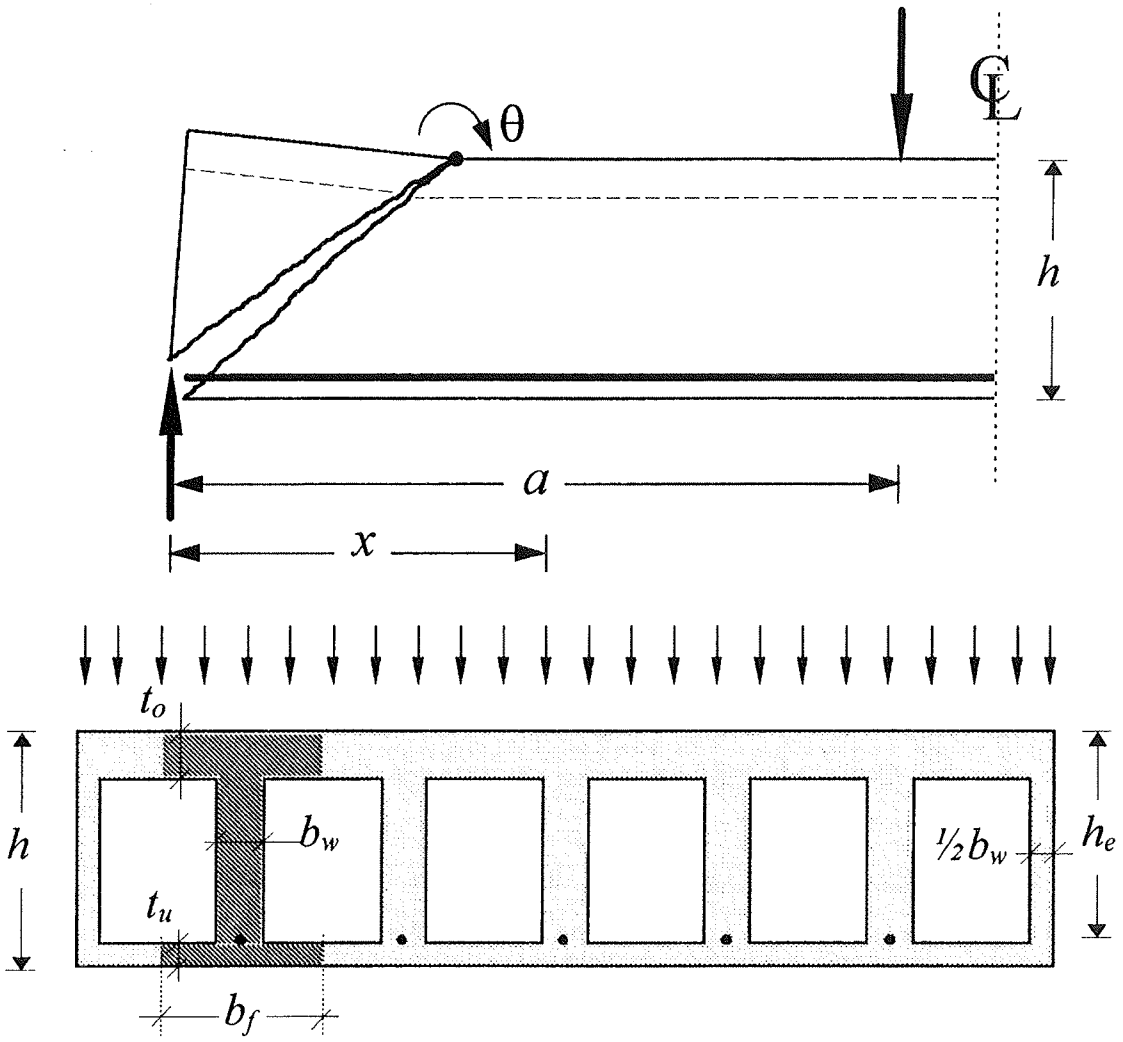

Figure 3.5 *Cross section of hollow-core slab in the case of rotation failure.*

Chapter 4

Comparison with Test Results

In order to verify the derived formulas for the shear capacity of prestressed hollow-core slabs, four test series have been investigated.

The four test series, which all together comprise 159 tests failed in shear, are from the references [82.1], [83.1] and [90.1].

Information about the diameter of the strands were only available for the tests reported in [83.1]. For these tests the transfer length was taken as 55ϕ. In the other cases the transfer length has been chosen at 600 mm.

For all the tests, the quantities t_o, t_u and b_w have been determined as outlined in the introduction of chapter 3. In the cases where no measures were given, the necessary quantities were measured on the drawings available.

Data concerning the test results and the calculated shear capacities can be found in the appendix A, B, C and D.

4.1 Tests from Delft University of Technology

This test series was carried out at Delft University of Technology (DUT) and has been reported by Walraven el al [83.1]. The test specimens were loaded by a single line load, which was asymmetrical with respect to the span middle. The load was applied through a rigid transverse steel beam. Slabs with three different cross sections were tested, see figure 4.1.

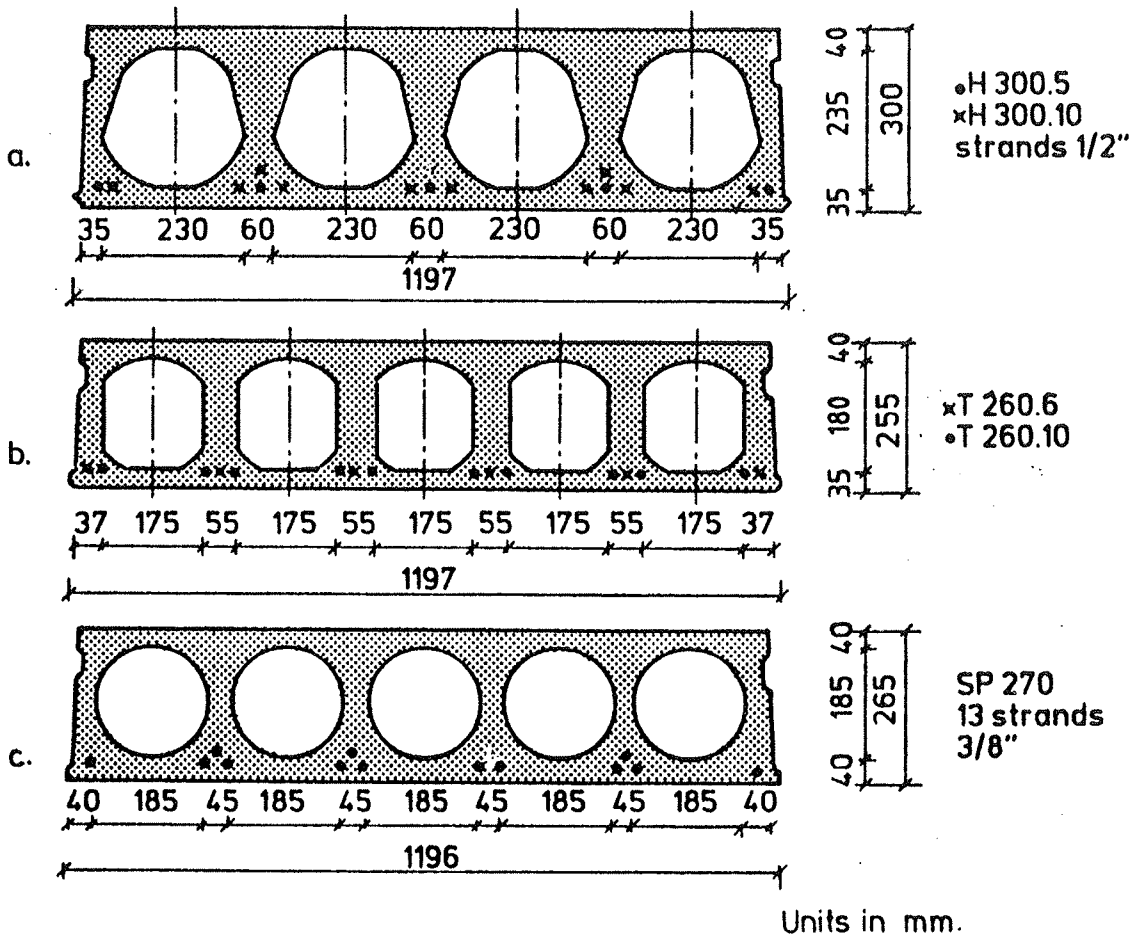

Figure 4.1 *Cross sections of the elements tested at DUT.*

The comparison between tests and theory has been shown in figure 4.2. The mean value of the ratio $V_{test}/V_{cal.}$ is 1.08 and the standard deviation is 0.11.

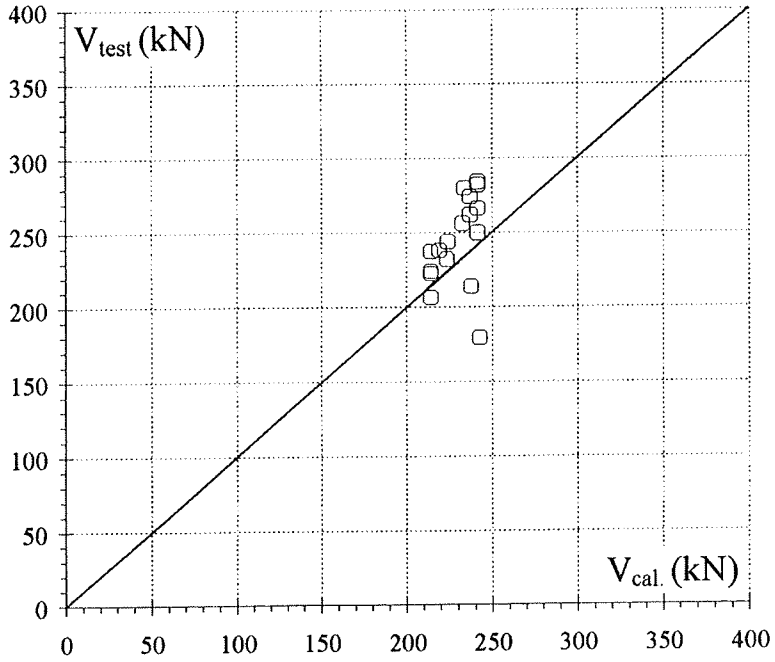

Figure 4.2 *Comparison of theory with test results from DUT* [*83.1*].

4.2 Tests from CBR in Belgium

These tests were carried out at the laboratory of CBR, and the results are reported in [82.1]. The test arrangement and the cross sections are shown in figure 4.3. Eccentrical loading were prevented by a hinged support.

The effective prestressing level was, as described in [82.1], 65% of the strength of the strands, which was 1860 MPa. Here the losses of prestress due to elastic shortening, relaxation, shrinkage and creep have been taken into account.

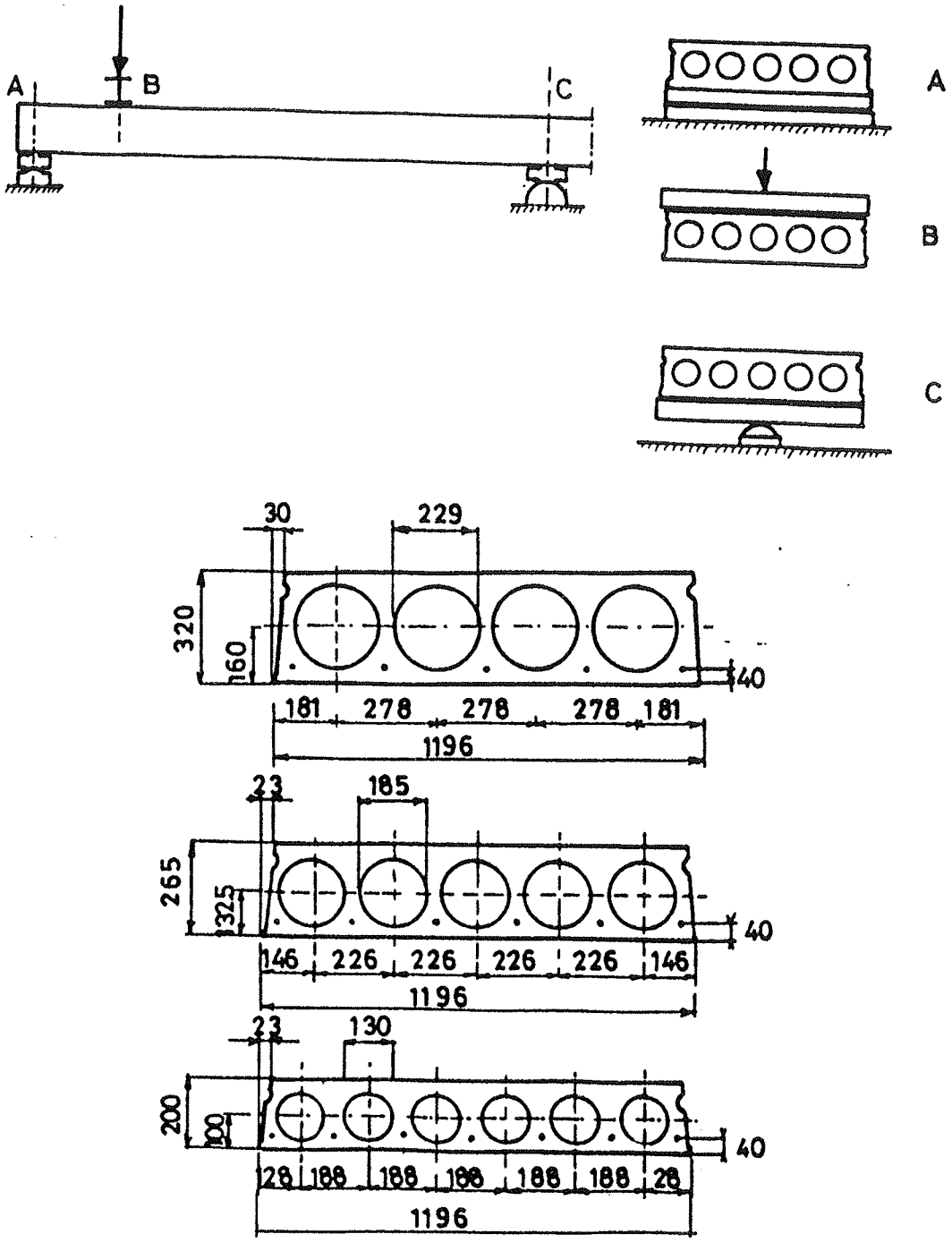

Figure 4.3 *Test arrangement and cross sections of the elements tested at CBR.*

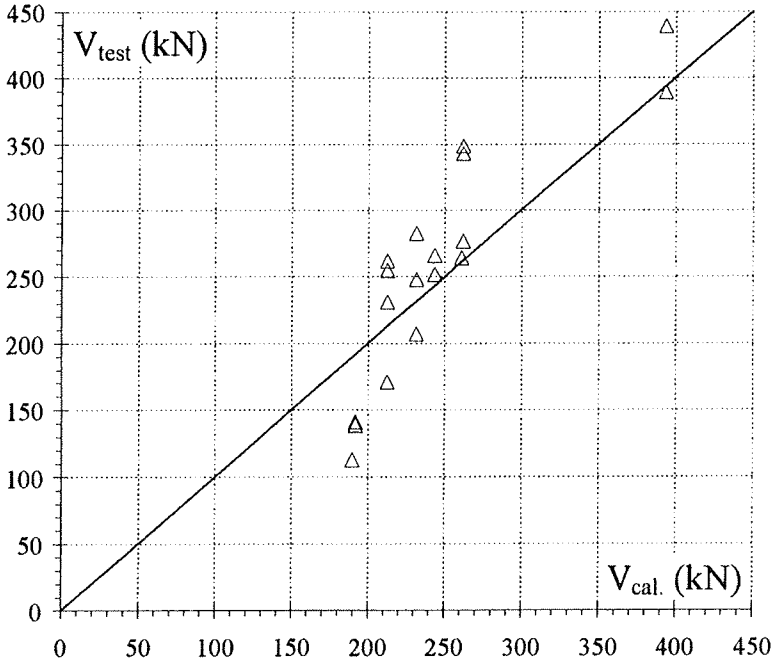

Figure 4.4 *Comparison of theory with test results from CBR* [*82.1*].

The comparison between tests and theory is shown in figure 4.4. In this case the mean value of the ratio $V_{test}/V_{cal.}$ is found to be 1.04 while the standard deviation is 0.21.

4.3 Tests from Einhoven University of Technology

The test arrangement and the cross sections of the elements tested at Einhoven University of Technology (TUE) can be seen in figure 4.5. Data concerning these tests may also be found in reference [82.1].

For this particular test series, the top of the slabs were also provided with a small amount of prestressing reinforcement (104 mm^2), which was placed in a distance of 35mm from the upper side. However, in the calculation of the cracking load, the contribution from these prestressing strands was disregarded due to the small lever arm.

As reported in [82.1] there were some doubts concerning the way the compressive strength of concrete was determined. The compaction of the concrete in the cube moulds may not have been the same as the compaction of the slabs obtained by the extruding machine[1)].

Due to these uncertainties it was decided, as reported in [82.1], to use the value f_{cc} = 65 MPa for all tests. This value has also been used in the present calculations.

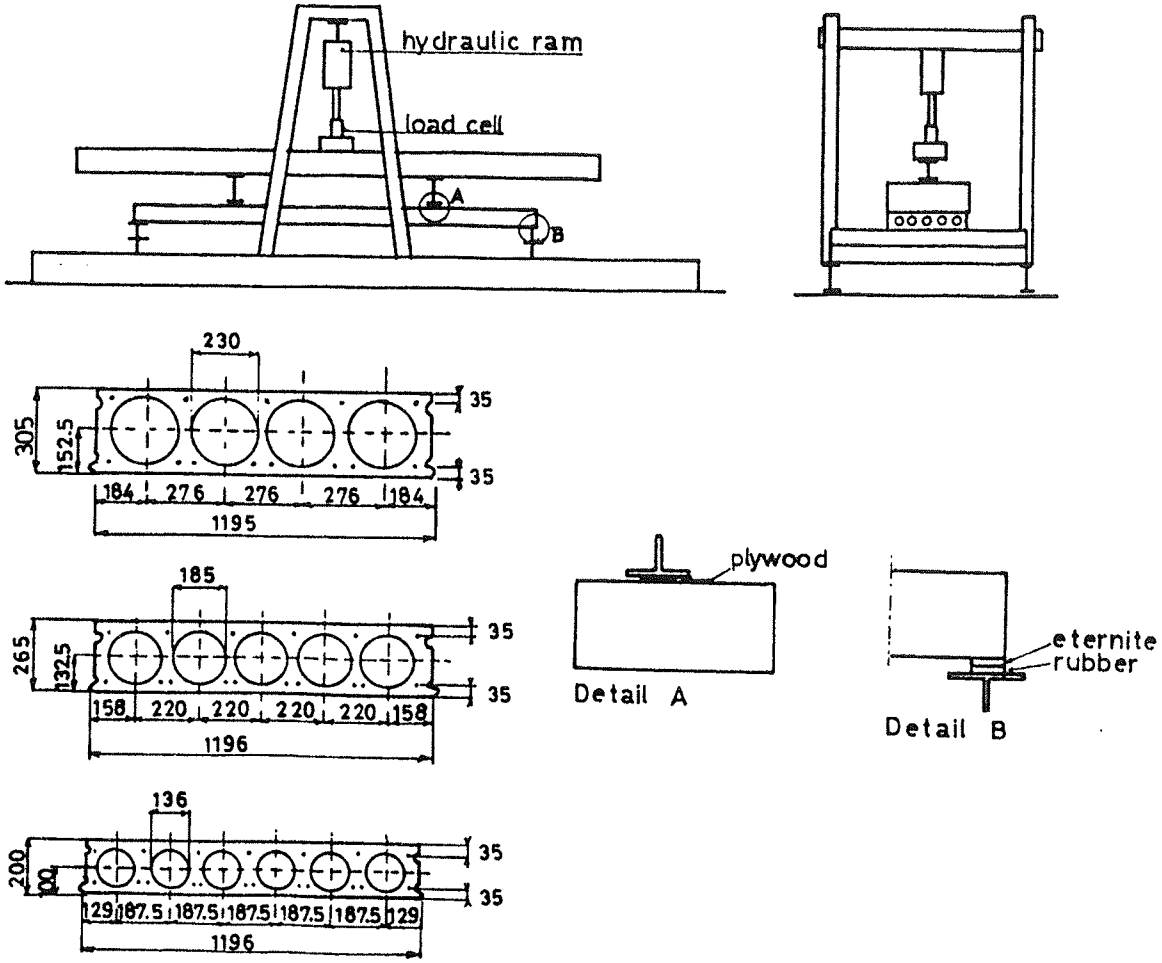

Figure 4.5 *Test arrangement and cross sections of the elements tested at TUE.*

[1)] Some slabs with identical properties, except a significant difference in cube strength, had approximately the same shear strength.

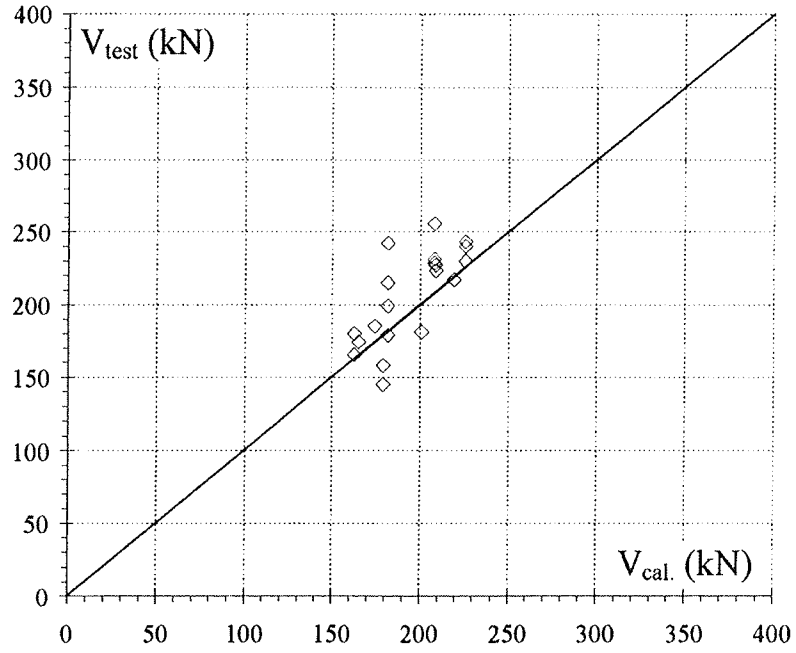

Figure 4.6 *Comparison of theory with test results from TUE [82.1].*

The comparison between theory and tests is shown in figure 4.6. The mean value of the ratio V_{test}/V_{cal} is found to be 1.08 while the standard deviation is 0.12.

4.4 Tests from Dansk Spændbeton

This test series from Dansk Spændbeton [90.1] consists of 103 test results. The test arrangement and the cross section are shown in figure 4.7.

The producer of the slabs informed that the effective prestressing force in a $\frac{1}{2}$" strand may be taken as 110 kN. Since the cross section area of such a strand is 98.7 mm^2 and the strength is f_p=1800 MPa, the prestressing level is found to be 62% of the strength of the strands.

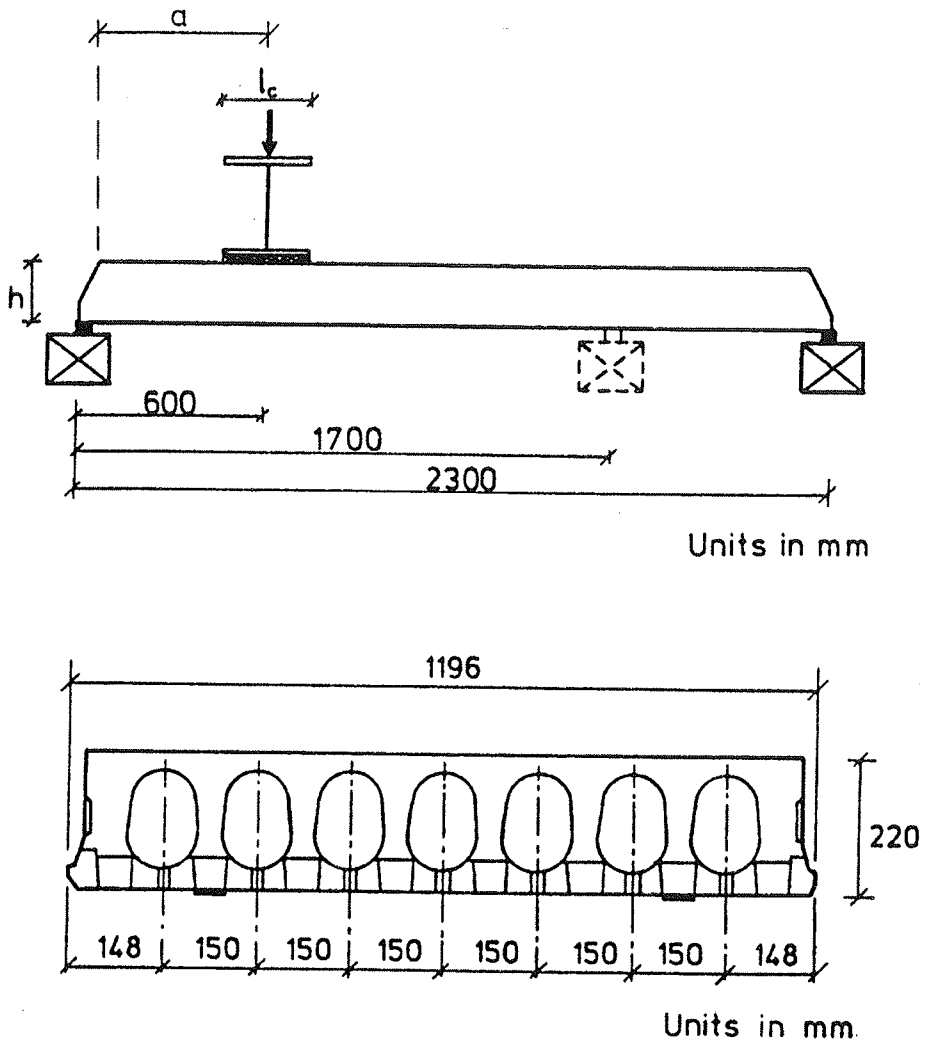

Figure 4.7 *Test arrangement and cross section of the elements tested at Dansk Spændbeton.*

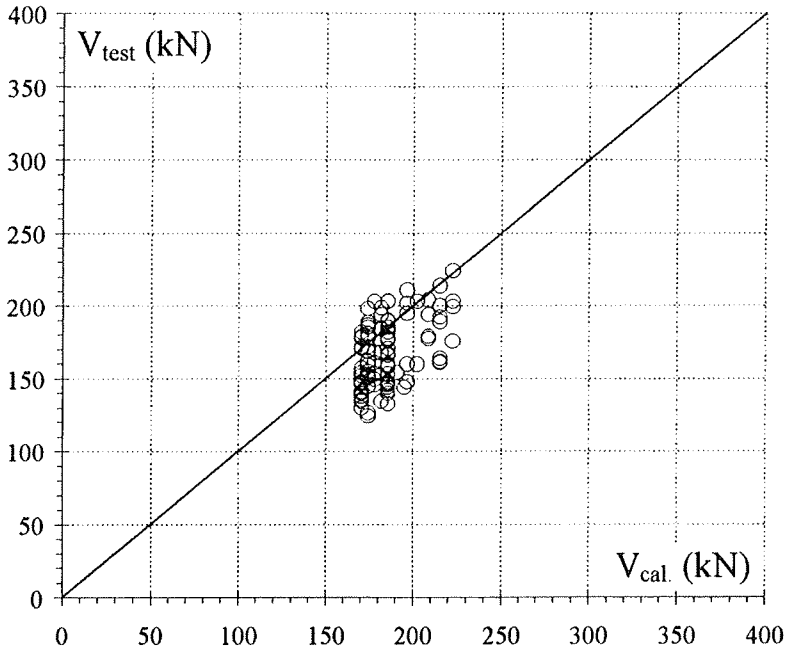

Figure 4.8 *Comparison of theory with test results from Dansk spændbeton* [*90.1*].

The comparison between theory and tests is shown in figure 4.8. The mean value of the ratio V_{test}/V_{cal} is 0.90 and the standard deviation is 0.11.

4.5 Comparison with all tests

The 159 test results from the four series are combined in figure 4.9.

All together, the mean value of V_{test}/V_{cal} is found to be 0.96 and the standard deviation is 0.15.

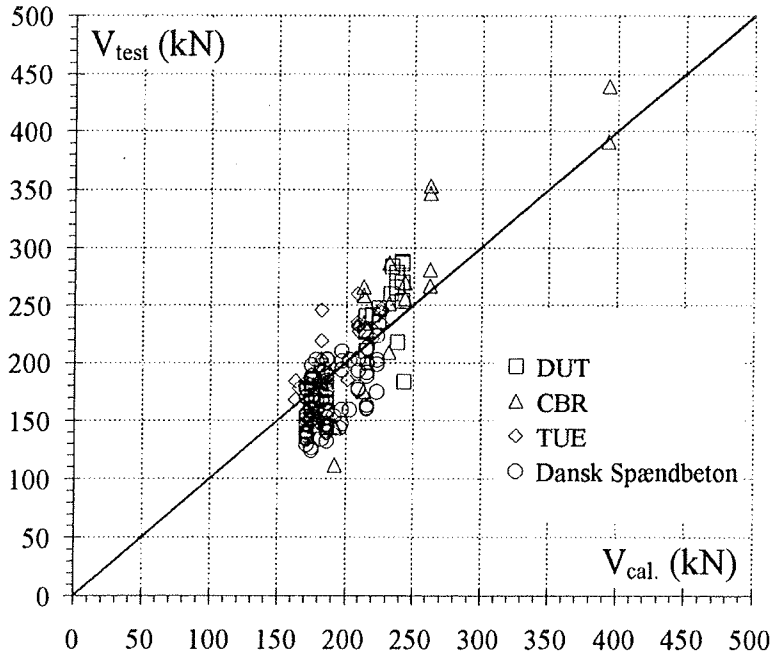

Figure 4.9 *Comparison of theory with 159 test results.*

Chapter 5

Conclusion

This report has been dealing with the shear capacity of prestressed hollow-core slabs determined by the theory of plasticity. The solutions were derived by considering two failure mechanisms.

In the first case, sliding in cracks was considered and the solution was found according to the crack sliding model developed by Jin-Ping Zhang [94.1]. The special assumptions/conditions which were introduced in order to derive this solution are as follows:

1) The area of the compression flange is disregarded. 2) The prestressing reinforcement does not yield at failure and is capable of maintaining moment equilibrium after the formation of the critical diagonal crack. 3) The pre-stressing force varies linearly in the transfer zone.

In the second case, a rotation mechanism induced by a crack formed at the support was considered. The solution was derived under the assumption that slip of strands occurs.

The theoretical results have been compared with 159 test results found in the literature. Good agreement was found.

References

[78.1] Nielsen, M.P. & Bræstrup, M.W. & Jensen, B.C. & Bach, F. : *Concrete Plasticity----Beam shear-Shear in joints-Punching shear.* Special Publication. Danish Society for Structural Science and Engineering, Structural Research Laboratory, Technical University of Denmark, Lyngby, 1978.

[79.1] Mianowski, K. : *The bearing capacity and the failure mechanism of hollow-core slabs in combined bending and shear.* Report 79:3. Division of Concrete Structures, Chalmers University of Technology, Göteborg, 1979.

[82.1] Walraven, J.C. et al : *Design principles for hollow core-slabs regarding shear and transverse load bearing capacity, splitting and quality control.* FIP Technical Paper, October 1982.

[83.1] Walraven, J.C. & Mercx, W.P.M. :
The bearing capacity for prestressed hollow-core slabs.
Heron, Vol. 28, No. 3. Delft University of Technology, The Netherlands, 1983.

[84.1] Nielsen, M. P. :
Limit analysis and concrete plasticity.
Prentice-Hall, Inc. Englewood Cliffs, NewJersey, 1984.

[86.1] Larsen, H. :
Huldæk- og væg-elementer i beton. Bæreevnebestemmelse. (Concrete hollow-core slabs and wall elements. Determination of load carrying capacity).
Technical University of Denmark, Institute of Building Design. Report No. 70 , Lyngby, 1986.

[90.1] Olsen, D.H. & Ganwei, C. & Nielsen, M. P. :
Plastic shear solutions of prestressed hollow-core concrete slabs.
Technical University of Denmark, Department of Structural Engineering, Report R No. 257, Lyngby, 1990.

[94.1] Zhang, Jin-Ping :
Strength of cracked concrete. Part 1--- Shear strength of conventional reinforced concrete beams, deep beams, corbels, and prestressed reinforced concrete beams without shear reinforcement.
Technical University of Denmark , Department of Structural Engineering, Report R No. 311, Lyngby, 1994.

[94.2] Yang, Lin :
Design of prestressed hollow-core slabs with reference to web shear failure.
Journal of Structural Engineering. Vol. 120, No. 9, September 1994.

[96.1] Zhang, Jin-Ping :
Strength of cracked concrete. Part 2--- Micromechanical modelling of shear failure in cement paste and in concrete.
Technical University of Denmark , Department of Structural Engineering and Materials, Report R No. 17, Lyngby, 1997.

[96.2] Engström, Björn :
Beräkning av förspända betongkonstruktioner.(Analysis of prestressed concrete structures).
Division of Concrete Structures, Chalmers University of Technology, Göteborg, 1996.

[97.1] Nielsen, M. P. :
Limit analysis and concrete plasticity. Second edition (to be published).

[97.2] Hoang, Cao Linh :
Shear strength of non-shear reinforced concrete elements. Part 1. Statically indeterminate beams. Technical University of Denmark , Department of Structural Engineering and Materials, Report R No. 16, Lyngby, 1997.

[97.3] Hoang, Cao Linh :
Shear strength of non-shear reinforced concrete elements. Part 2. T- beams. Technical University of Denmark ,Department of Structural Engineering and Materials, (to be published).

Appendix A

Tests from Delft University of Technology [83.1]

No.	h	a/h	h_e/h	s	t_o	t_u	b_w	b_f	l_t	n	f_c	f_p	A_p	F_{se}	V_{test}	$V_{cal.}$ [1)]	$V_{cal.}$ [2)]
	mm			mm	mm	mm	mm	mm	mm		MPa	MPa	mm^2	kN	kN	kN	kN
T2615A	255	3.16	0.86	100	40	35	55	230	690	5	63.2	1800	564	648.6	234.2	221.7	248.0
T2615B	255	1.80	0.86	100	40	35	55	230	690	5	63.2	1800	564	648.6	258.3	230.9	248.0
T2616A	255	3.16	0.86	100	40	35	55	230	690	5	63.2	1800	654	648.6	245.9	222.4	248.0
T2616B	255	1.80	0.86	100	40	35	55	230	690	5	63.2	1800	654	648.6	282	231.8	248.0
T2604A	255	1.80	0.86	100	40	35	55	230	690	5	60	1800	940	1081	284.3	275.5	239.5
T2604B	255	3.16	0.86	100	40	35	55	230	690	5	60	1800	940	1081	268.3	308.7	239.5
T2605A	255	1.80	0.86	100	40	35	55	230	690	5	60	1800	940	1081	286.3	275.5	239.5
T2605B	255	4.51	0.86	100	40	35	55	230	690	5	60	1800	940	1081	252.1	255.3	239.5
P2718-	265	4.34	0.85	100	40	40	45	230	520	5	58.8	1800	676	777.3	240.3	217.3	235.3
P2719A	265	3.04	0.85	100	40	40	45	230	520	5	58.8	1800	676	777.3	276.3	286.6	235.3
P2719B	265	1.74	0.85	100	40	40	45	230	520	5	58.8	1800	676	777.3	263.9	274.5	235.3
H3007A	300	1.80	0.88	100	35	35	60	290	690	4	67.7	1800	470	540.5	216	235.8	254.2
H3008B	300	1.47	0.88	100	35	35	60	290	690	4	67.7	1800	470	540.5	181.6	240.9	254.2
H3010A	300	1.80	0.88	100	35	35	60	290	690	4	51.7	1800	940	1081	208.5	226.7	212.4
H3011A	300	3.15	0.88	100	35	35	60	290	690	4	51.7	1800	940	1081	224.6	226.7	212.4
H3011B	300	1.80	0.88	100	35	35	60	290	690	4	51.7	1800	940	1081	239.3	226.7	212.4
H3012-	300	4.98	0.88	100	35	35	60	290	690	4	51.7	1800	940	1081	226.2	238.3	212.4

[1)] Calculated shear capacity corresponding to sliding failure.

[2)] Calculated shear capacity corresponding to rotation failure.

Appendix B

Tests from CBR in Belgium [82.1]

No.	h	a/h	h_e/h	s	t_o	t_u	b_w	b_f	l_t	n	f_c	f_p	A_p	F_{se}	V_{test}	$V_{cal.}$ [1)]	$V_{cal.}$ [2)]
	mm			mm	mm	mm	mm	mm	mm		MPa	MPa	mm^2	kN	kN	kN	kN
15	200	2.50	0.8	40	35	35	58	188	600	6	65	1860	260	314.8	109	189.7	254.4
16	200	2.50	0.8	40	35	35	58	188	600	6	65	1860	260	314.8	141	189.7	254.4
17	200	2.50	0.8	90	35	35	58	188	600	6	65	1860	260	314.8	143	189.7	254.4
21	200	2.50	0.8	40	35	35	58	188	600	6	65	1860	624	755.5	207	229.7	254.4
22	200	2.50	0.8	40	35	35	58	188	600	6	65	1860	624	755.5	250	229.7	254.4
24	200	2.50	0.8	90	35	35	58	188	600	6	65	1860	624	755.5	285	229.7	254.4
25	265	2.50	0.85	40	40	40	41	226	600	5	65	1860	416	503.7	233	210.7	241.5
26	265	2.50	0.85	40	40	40	41	226	600	5	65	1860	416	503.7	173	210.7	241.5
27	265	2.50	0.85	90	40	40	41	226	600	5	65	1860	416	503.7	257	210.7	241.5
28	265	2.50	0.85	90	40	40	41	226	600	5	65	1860	416	503.7	264	210.7	241.5
29	265	2.50	0.85	40	40	40	41	226	600	5	65	1860	728	881.5	254	294.5	241.5
30	265	2.50	0.85	40	40	40	41	226	600	5	65	1860	728	881.5	268	294.5	241.5
35	320	2.50	0.78	40	45.5	45.5	49	278	600	4	65	1860	832	1007	279	367.5	259.8
36	320	2.5	0.78	40	45.5	45.5	49	278	600	4	65	1860	832	1007	265	367.5	259.8
37	320	2.5	0.78	90	45.5	45.5	49	278	600	4	65	1860	832	1007	345	367.5	259.8
38	320	2.5	0.78	90	45.5	45.5	49	278	600	4	65	1860	832	1007	351	367.5	259.8
39	320	2.5	0.78	**	45.5	45.5	49	278	600	4	65	1860	832	1007	441	391.6	**
40	320	2.5	0.78	**	45.5	45.5	49	278	600	4	65	1860	832	1007	391	391.6	**

[1)] Calculated shear capacity corresponding to sliding failure.

[2)] Calculated shear capacity corresponding to rotation failure.

[**)] For these two tests the support plates were placed in a distance 1000 mm from the edge of the slab.

Appendix C

Tests from Einhoven University of Technology [82.1]

No.	h	a/h	h_e/h	s	t_o	t_u	b_w	b_f	l_t	n	f_c	f_p	A_p *)	F_{se}	V_{test}	$V_{cal.}$ 1)	$V_{cal.}$ 2)
	mm			mm	mm	mm	mm	mm	mm		MPa	MPa	mm^2	kN	kN	kN	kN
21	200	6	0.825	100	32	32	51.5	187.5	600	6	65	1860	640	775.0	147	174.4	233.5
22	200	6	0.825	100	32	32	51.5	187.5	600	6	65	1860	640	775.0	156.3	174.4	233.5
1	265	3.58	0.87	100	40	40	35	220	600	5	65	1860	268	324.5	176.3	163.2	226.6
33	265	3.58	0.87	100	40	40	35	220	600	5	65	1860	640	775.0	241.9	248.0	226.6
34	265	3.58	0.87	100	40	40	35	220	600	5	65	1860	640	775.0	231.8	248.0	226.6
35	265	3.58	0.87	100	40	40	35	220	600	5	65	1860	640	775.0	245.1	248.0	226.6
10	265	4.5	0.87	100	40	40	35	220	600	5	65	1860	640	775.0	225.2	207.4	226.6
11	265	4.53	0.87	100	40	40	35	220	600	5	65	1860	640	775.0	233.2	206.4	226.6
12	265	4.51	0.87	100	40	40	35	220	600	5	65	1860	640	775.0	229.2	207.1	226.6
13	265	4.53	0.87	100	40	40	35	220	600	5	65	1860	640	775.0	230.4	206.4	226.6
14	265	4.53	0.87	100	40	40	35	220	600	5	65	1860	640	775.0	257.8	206.4	226.6
9	265	5.47	0.87	100	40	40	35	220	600	5	65	1860	640	775.0	243.9	179.8	226.6
41	265	5.47	0.87	100	40	40	35	220	600	5	65	1860	640	775.0	181	179.8	226.6
43	265	5.47	0.87	100	40	40	35	220	600	5	65	1860	640	775.0	217.7	179.8	226.6
44	265	5.47	0.87	100	40	40	35	220	600	5	65	1860	640	775.0	201.2	179.8	226.6
39	265	6.42	0.87	100	40	40	35	220	600	5	65	1860	640	775.0	166.3	160.9	226.6
40	265	6.42	0.87	100	40	40	35	220	600	5	65	1860	640	775.0	182	160.9	226.6
36	305	4.61	0.89	100	38	38	46	276	600	4	65	1860	733	887.6	219	223.3	217.5
38	305	5.34	0.89	100	38	38	46	276	600	4	65	1860	733	887.6	183.2	199.2	217.5
37	305	6.49	0.89	100	38	38	46	276	600	4	65	1860	733	887.6	187.3	172.5	217.5

1) Calculated shear capacity corresponding to sliding failure.

2) Calculated shear capacity corresponding to rotation failure.

*) Additional to the reinforcement given in the table, all the elements from this series contained a prestressing reinforcement of 104 mm^2 at a distance of 35 mm from the upper face.

Appendix D

Tests from Dansk Spændbeton [90.1]

No.	h	a/h	h_e/h	s	t_o	t_u	b_w	b_f	l_t	n	f_c	f_p	A_p	F_{se}	V_{test}	$V_{cal.}$ [1)]	$V_{cal.}$ [2)]
	mm			mm	mm	mm	mm	mm	mm		MPa	MPa	mm^2	kN	kN	kN	kN
1	220	2.73	0.82	-	35	35	44	150	600	7	58	1800	288	321.4	144	168.8	220.9
2	220	2.73	0.82	-	35	35	44	150	600	7	58	1800	416	464.3	173.4	183.8	220.9
3	220	2.73	0.82	-	35	35	44	150	600	7	58	1800	416	464.3	139.2	183.8	220.9
4	220	2.73	0.82	-	35	35	44	150	600	7	58	1800	416	464.3	157.2	183.8	220.9
5	220	2.73	0.82	-	35	35	44	150	600	7	58	1800	320	357.1	159	172.4	220.9
6	220	2.73	0.82	-	35	35	44	150	600	7	58	1800	457	510.0	151.8	189.2	220.9
7	220	2.73	0.82	-	35	35	44	150	600	7	58	1800	320	357.1	148.2	172.4	220.9
8	220	2.73	0.82	-	35	35	44	150	600	7	58	1800	498	555.8	192	194.8	220.9
9	220	2.73	0.82	-	35	35	44	150	600	7	58	1800	416	464.3	200.4	183.8	220.9
10	220	2.73	0.82	-	35	35	44	150	600	7	58	1800	384	428.5	181.2	179.9	220.9
11	220	2.73	0.82	-	35	35	44	150	600	7	58	1800	384	428.5	181.8	179.9	220.9
12	220	2.73	0.82	-	35	35	44	150	600	7	58	1800	416	464.3	144	183.8	220.9
13	220	2.73	0.82	-	35	35	44	150	600	7	58	1800	416	464.3	157.2	183.8	220.9
14	220	2.73	0.82	-	35	35	44	150	600	7	58	1800	416	464.3	187.8	183.8	220.9
15	220	2.73	0.82	-	35	35	44	150	600	7	58	1800	498	555.8	208.2	194.8	220.9
16	220	2.73	0.82	-	35	35	44	150	600	7	58	1800	416	464.3	157.2	183.8	220.9
17	220	2.73	0.82	-	35	35	44	150	600	7	58	1800	416	464.3	157.2	183.8	220.9
18	220	2.73	0.82	-	35	35	44	150	600	7	58	1800	384	428.5	196.2	179.9	220.9

[1)] Calculated shear capacity corresponding to sliding failure.

[2)] Calculated shear capacity corresponding to rotation failure.

Tests from Dansk Spændbeton [90.1] (continued)

No.	h	a/h	h_e/h	s	t_o	t_u	b_w	b_f	l_t	n	f_c	f_p	A_p	F_{se}	V_{test}	$V_{cal.}$ [1]	$V_{cal.}$ [2]
19	220	2.73	0.82	-	35	35	44	150	600	7	58	1800	416	464.3	144	183.8	220.9
20	220	2.73	0.82	-	35	35	44	150	600	7	58	1800	416	464.3	186.6	183.8	220.9
21	220	2.73	0.82	-	35	35	44	150	600	7	58	1800	498	555.8	157.2	194.8	220.9
22	220	2.73	0.82	-	35	35	44	150	600	7	58	1800	744	830.3	221.4	235.2	220.9
23	220	2.73	0.82	-	35	35	44	150	600	7	58	1800	352	392.8	165	176.0	220.9
24	220	2.73	0.82	-	35	35	44	150	600	7	58	1800	416	464.3	164.4	183.8	220.9
25	220	2.73	0.82	-	35	35	44	150	600	7	58	1800	416	464.3	130.2	183.8	220.9
26	220	2.73	0.82	-	35	35	44	150	600	7	58	1800	320	357.1	142.2	172.4	220.9
27	220	2.73	0.82	-	35	35	44	150	600	7	58	1800	498	555.8	145.2	194.8	220.9
28	220	2.73	0.82	-	35	35	44	150	600	7	58	1800	320	357.1	169.2	172.4	220.9
29	220	2.73	0.82	-	35	35	44	150	600	7	58	1800	352	392.8	143.4	176.0	220.9
30	220	2.73	0.82	-	35	35	44	150	600	7	58	1800	352	392.8	151.2	176.0	220.9
31	220	2.73	0.82	-	35	35	44	150	600	7	58	1800	288	321.4	135.6	168.8	220.9
32	220	2.73	0.82	-	35	35	44	150	600	7	58	1800	416	464.3	145.2	183.8	220.9
33	220	2.73	0.82	-	35	35	44	150	600	7	58	1800	384	428.5	191.4	179.9	220.9
34	220	2.73	0.82	-	35	35	44	150	600	7	58	1800	744	830.3	172.8	235.2	220.9
35	220	2.73	0.82	-	35	35	44	150	600	7	58	1800	320	357.1	148.8	172.4	220.9
36	220	2.73	0.82	-	35	35	44	150	600	7	58	1800	416	464.3	174.6	183.8	220.9
37	220	2.73	0.82	-	35	35	44	150	600	7	58	1800	288	321.4	137.4	168.8	220.9
38	220	2.73	0.82	-	35	35	44	150	600	7	58	1800	744	830.3	196.8	235.2	220.9
39	220	2.73	0.82	-	35	35	44	150	600	7	58	1800	416	464.3	141.6	183.8	220.9
40	220	2.73	0.82	-	35	35	44	150	600	7	58	1800	580	647.3	176.4	206.9	220.9
41	220	2.73	0.82	-	35	35	44	150	600	7	58	1800	539	601.5	200.4	200.7	220.9
42	220	2.73	0.82	-	35	35	44	150	600	7	58	1800	416	464.3	155.4	183.8	220.9
43	220	2.73	0.82	-	35	35	44	150	600	7	58	1800	352	392.8	158.4	176.0	220.9

[1] Calculated shear capacity corresponding to sliding failure.

[2] Calculated shear capacity corresponding to rotation failure.

Tests from Dansk Spændbeton [90.1] (continued)

No.	h	a/h	h_e/h	s	t_o	t_u	b_w	b_f	l_t	n	f_c	f_p	A_p	F_{se}	V_{test}	$V_{cal.}$ [1)]	$V_{cal.}$ [2)]
44	220	2.73	0.82	-	35	35	44	150	600	7	58	1800	580	647.3	201.6	206.9	220.9
45	220	2.73	0.82	-	35	35	44	150	600	7	58	1800	621	693.0	189.6	213.5	220.9
46	220	2.73	0.82	-	35	35	44	150	600	7	58	1800	320	357.1	184.2	172.4	220.9
47	220	2.73	0.82	-	35	35	44	150	600	7	58	1800	416	464.3	200.4	183.8	220.9
48	220	2.73	0.82	-	35	35	44	150	600	7	58	1800	288	321.4	151.8	168.8	220.9
49	220	2.73	0.82	-	35	35	44	150	600	7	58	1800	320	357.1	195.6	172.4	220.9
50	220	2.73	0.82	-	35	35	44	150	600	7	58	1800	320	357.1	186	172.4	220.9
51	220	2.73	0.82	-	35	35	44	150	600	7	58	1800	352	392.8	147	176.0	220.9
52	220	2.73	0.82	-	35	35	44	150	600	7	58	1800	288	321.4	133.2	168.8	220.9
53	220	2.73	0.82	-	35	35	44	150	600	7	58	1800	288	321.4	145.2	168.8	220.9
54	220	2.73	0.82	-	35	35	44	150	600	7	58	1800	416	464.3	182.4	183.8	220.9
55	220	2.73	0.82	-	35	35	44	150	600	7	58	1800	288	321.4	149.4	168.8	220.9
56	220	2.73	0.82	-	35	35	44	150	600	7	58	1800	352	392.8	150.6	176.0	220.9
57	220	2.73	0.82	-	35	35	44	150	600	7	58	1800	288	321.4	149.4	168.8	220.9
58	220	2.73	0.82	-	35	35	44	150	600	7	58	1800	416	464.3	168	183.8	220.9
59	220	2.73	0.82	-	35	35	44	150	600	7	58	1800	416	464.3	137.4	183.8	220.9
60	220	2.73	0.82	-	35	35	44	150	600	7	58	1800	320	357.1	175.2	172.4	220.9
61	220	2.73	0.82	-	35	35	44	150	600	7	58	1800	320	357.1	124.2	172.4	220.9
62	220	2.73	0.82	-	35	35	44	150	600	7	58	1800	416	464.3	150.6	183.8	220.9
63	220	2.73	0.82	-	35	35	44	150	600	7	58	1800	320	357.1	166.2	172.4	220.9
64	220	2.73	0.82	-	35	35	44	150	600	7	58	1800	288	321.4	145.2	168.8	220.9
65	220	2.73	0.82	-	35	35	44	150	600	7	58	1800	580	647.3	191.4	206.9	220.9

[1)] Calculated shear capacity corresponding to sliding failure.

[2)] Calculated shear capacity corresponding to rotation failure.

Tests from Dansk Spændbeton [90.1] (continued)

No.	h	a/h	h_e/h	s	t_o	t_u	b_w	b_f	l_t	n	f_c	f_p	A_p	F_{se}	V_{test}	$V_{cal.}$ [1)]	$V_{cal.}$ [2)]
66	220	2.73	0.82	-	35	35	44	150	600	7	58	1800	288	321.4	127.2	168.8	220.9
67	220	2.73	0.82	-	35	35	44	150	600	7	58	1800	621	693.0	186.6	213.5	220.9
68	220	2.73	0.82	-	35	35	44	150	600	7	58	1800	288	321.4	168.6	168.8	220.9
69	220	2.73	0.82	-	35	35	44	150	600	7	58	1800	621	693.0	197.4	213.5	220.9
70	220	2.73	0.82	-	35	35	44	150	600	7	58	1800	288	321.4	132	168.8	220.9
71	220	2.73	0.82	-	35	35	44	150	600	7	58	1800	416	464.3	163.2	183.8	220.9
72	220	2.73	0.82	-	35	35	44	150	600	7	58	1800	288	321.4	176.4	168.8	220.9
73	220	2.73	0.82	-	35	35	44	150	600	7	58	1800	744	830.3	200.4	235.2	220.9
74	220	2.73	0.82	-	35	35	44	150	600	7	58	1800	288	321.4	138.6	168.8	220.9
75	220	2.73	0.82	-	35	35	44	150	600	7	58	1800	621	693.0	211.2	213.5	220.9
76	220	2.73	0.82	-	35	35	44	150	600	7	58	1800	288	321.4	168.6	168.8	220.9
77	220	2.73	0.82	-	35	35	44	150	600	7	58	1800	416	464.3	179.4	183.8	220.9
78	220	2.73	0.82	-	35	35	44	150	600	7	58	1800	621	693.0	161.4	213.5	220.9
79	220	2.73	0.82	-	35	35	44	150	600	7	58	1800	320	357.1	178.2	172.4	220.9
80	220	2.73	0.82	-	35	35	44	150	600	7	58	1800	621	693.0	158.4	213.5	220.9
81	220	2.73	0.82	-	35	35	44	150	600	7	58	1800	416	464.3	175.2	183.8	220.9
82	220	2.73	0.82	-	35	35	44	150	600	7	58	1800	320	357.1	152.4	172.4	220.9
83	220	2.73	0.82	-	35	35	44	150	600	7	58	1800	288	321.4	154.2	168.8	220.9
84	220	2.73	0.82	-	35	35	44	150	600	7	58	1800	320	357.1	156.6	172.4	220.9
85	220	2.73	0.82	-	35	35	44	150	600	7	58	1800	288	321.4	168	168.8	220.9
86	220	2.73	0.82	-	35	35	44	150	600	7	58	1800	416	464.3	201	183.8	220.9
87	220	2.73	0.82	-	35	35	44	150	600	7	58	1800	352	392.8	200.4	176.0	220.9
88	220	2.73	0.82	-	35	35	44	150	600	7	58	1800	320	357.1	182.4	172.4	220.9
89	220	2.73	0.82	-	35	35	44	150	600	7	58	1800	288	321.4	175.2	168.8	220.9

[1)] Calculated shear capacity corresponding to sliding failure.

[2)] Calculated shear capacity corresponding to rotation failure.

Tests from Dansk Spændbeton [90.1] (continued)

No.	h	a/h	h_e/h	s	t_o	t_u	b_w	b_f	l_t	n	f_c	f_p	A_p	F_{sc}	V_{test}	$V_{cal.}$ [1)]	$V_{cal.}$ [2)]
90	220	2.73	0.82	-	35	35	44	150	600	7	58	1800	416	464.3	200.4	183.8	220.9
91	220	2.73	0.82	-	35	35	44	150	600	7	58	1800	416	464.3	179.4	183.8	220.9
92	220	2.73	0.82	-	35	35	44	150	600	7	58	1800	621	693.0	159	213.5	220.9
93	220	2.73	0.82	-	35	35	44	150	600	7	58	1800	288	321.4	179.4	168.8	220.9
94	220	2.73	0.82	-	35	35	44	150	600	7	58	1800	580	647.3	174.6	206.9	220.9
95	220	2.73	0.82	-	35	35	44	150	600	7	58	1800	416	464.3	143.4	183.8	220.9
96	220	2.73	0.82	-	35	35	44	150	600	7	58	1800	416	464.3	156.6	183.8	220.9
97	220	2.73	0.82	-	35	35	44	150	600	7	58	1800	320	357.1	121.8	172.4	220.9
98	220	2.73	0.82	-	35	35	44	150	600	7	58	1800	320	357.1	150	172.4	220.9
99	220	2.73	0.82	-	35	35	44	150	600	7	58	1800	384	428.5	165	179.9	220.9
100	220	2.73	0.82	-	35	35	44	150	600	7	58	1800	498	555.8	199.2	194.8	220.9
101	220	2.73	0.82	-	35	35	44	150	600	7	58	1800	384	428.5	132	179.9	220.9
102	220	2.73	0.82	-	35	35	44	150	600	7	58	1800	539	601.5	157.2	200.7	220.9
103	220	2.73	0.82	-	35	35	44	150	600	7	58	1800	487	543.5	141.6	193.2	220.9

[1)] Calculated shear capacity corresponding to sliding failure.

[2)] Calculated shear capacity corresponding to rotation failure.